Mitochondrial dysfunction: unraveling the elusive biology behind anti-TNF response during ulcerative colitis

Dimitrios Kioroglou[1], Ainize Peña-Cearra[2,3], Ana M. Corraliza[4], Iratxe Seoane[2,3], Janire Castelo[2], Julian Panés[4,5], Laura Gómez-Irwin[6], Iago Rodríguez-Lago[7], Jone Ortiz de Zarate[8], Miguel Fuertes[10], Itziar Martín-Ruiz[2], Monika Gonzalez[9], Ana Mª Aransay[4,9], Azucena Salas[4], Héctor Rodríguez[2], Juan Anguita[2,11], Leticia Abecia[2,3,*], Urko M. Marigorta[1,11,*]

* Corresponding authors:
Leticia Abecia: leticia.abecia@ehu.eus
Urko M. Marigorta: umartinez@cicbiogune.es

Affiliation details
1. Integrative Genomics Lab, Center for Cooperative Research in Biosciences (CIC bioGUNE), Basque Research and Technology Alliance (BRTA), Bizkaia Technology Park, Derio, Basque Country, Spain.
2. Inflammation and Macrophage Plasticity Laboratory, CIC bioGUNE-BRTA (Basque Research and Technology Alliance), Derio 48160, Spain.
3. Immunology, Microbiology and Parasitology Department, Faculty of Medicine and Nursery, University of the Basque Country, UPV/EHU, P.O. Box 699, 48080 Bilbao, Spain.
4. Centro de Investigación Biomédica en Red de Enfermedades Hepática y Digestivas (CIBERehd), ISCIII, Barcelona, Spain.
5. Department of Gastroenterology, IDIBAPS, Hospital Clínic, Barcelona, Spain.
6. Hospital Universitario de Cruces and Biocruces Bizkaia Health Research Institute, 48903 Barakaldo, Spain.
7. Hospital Universitario de Galdakao and Biocruces Bizkaia Health Research Institute, 48960 Galdakao, Spain.
8. Hospital Universitario de Basurto. 48013 Bilbao, Bizkaia, Spain.
9. GAP, CIC bioGUNE-BRTA (Basque Research and Technology Alliance), Derio 48160, Spain.
10. NEIKER-Basque Institute for Agricultural Research and Development, Basque Research and Technology Alliance (BRTA), Bizkaia Science and Technology Park, Building 812L, 48160, Derio, Spain.
11. Ikerbasque, Basque Foundation for Science, 48013 Bilbao, Bizkaia, Spain.

Abbreviations

MM = colon samples from murine disease model
WT = all wild-type mice included in the MM dataset
WT-IFX$^-$ = wild-type mice without anti-TNF treatment
WT-IFX$^+$ = wild-type mice with anti-TNF treatment
MD = all mice of MM with MCJ-deficiency
MD-IFX$^-$ = mice with MCJ-deficiency and without anti-TNF treatment
MD-IFX$^+$ = mice with MCJ-deficiency and with anti-TNF treatment
MMset = 554 genes from MM that were differentially expressed between MD-IFX$^+$ and WT-IFX$^+$.
COL = colon samples at week-14 from a human cohort of responders and non-responders to anti-TNF UC patients.
COLset = 127 genes that intersected with MMset and were differentially expressed in the COL cohort.
HABset = 89 genes from Haberman *et al.* corticosteroid based gene signature that were differentially expressed in the COL cohort.
MON = monocyte samples of peripheral blood from a human cohort of healthy individuals and IBD patients.
MONset = 48 genes that intersected with COLset and were differentially expressed in the MON cohort.
BLD = whole blood samples at baseline (week-0) from a human cohort of responders and non-responders to anti-TNF UC patients.
BLDset = set of 14 genes that were used to classify response to anti-TNF from a whole blood sample at baseline.
PCA = principal component analysis
PCs = principal components
DEG = differentially expressed gene
DSS = dextran sodium sulfate

Abstract

Background: Recent studies hint at mitochondrial genes influencing UC patient response to anti-TNF treatment. We evaluated this hypothesis by following a targeted strategy to identify gene expression that captures the relationship between mitochondrial dysregulation and response to treatment. Our objective was to initially examine this relationship in colon samples and subsequently assess whether the resulting signal persists in the bloodstream.

Methods: We analyzed the transcriptome of colon samples from an anti-TNF treated murine model characterized by impaired mitochondrial activity and treatment resistance. We then transferred the findings that linked mitochondrial dysfunction and compromised treatment response to an anti-TNF treated UC human cohort. We next matched differential expression in the blood using monocytes from peripheral blood of controls and IBD patients, and we evaluated a classification process at baseline with whole blood samples from UC patients.

Results: In human colon samples, the derived gene-set from the murine model showed differential expression, primarily enriched metabolic pathways, and exhibited similar classification capacity as genes enriching inflammatory pathways. Moreover, the evaluation of the classification signal using blood samples from UC patients at baseline highlighted the involvement of mitochondrial homeostasis in treatment response.

Conclusion: Our results highlight the involvement of metabolic pathways and mitochondrial homeostasis in determining treatment response and their ability to provide promising classification signals with detection levels in both colon and bloodstream.

Introduction

Ulcerative colitis (UC) is an inflammatory bowel disease (IBD) of increasing worldwide incidence, characterized by relapsing and remitting periods. Lacking a definitive cure, the focus of treatments is to alleviate and control disease symptoms. Although current anti-TNF treatments can extend the remission periods, a considerable 10-30% of patients do not respond to the initial treatment, or lose their ability to respond (23-46%) over time [1].

Through comparisons of gene expression profiles of responder and non-responder patients, several genes with biomarker potential have been proposed. This includes intestinal Oncostatin M (OSM), IL13RA2 and TREM1, which were first identified using mucosal samples [2–4]. Similarly, Haberman *et al.* [5] provided a gene signature derived from rectal biopsies at baseline. Although originally described for response to corticosteroids, the gene signature had a similar efficiency on a cohort that received anti-TNF treatment, whereas reduced mitochondrial biogenesis was reported as an aggravating factor.

To avoid the invasive nature of the patient's monitoring via biopsies, identifying whole blood biomarkers is a priority. For instance, TREM1 expression is arising as a promising predictive biomarker, although the evidence is not yet conclusive [4,6]. In addition, a qPCR classifier aimed at classifying patients according to disease course is available [7].

In spite of the valuable endeavors towards classification solutions, current methodologies are based on differential gene expression analysis that lacks a perturbation source. To derive insights on the underlying mechanism and provide a gene signature that includes a reasonable number of differentially expressed genes (DEGs), studies resort to pathway enrichment analysis. However, this approach is based on using databases that may present

limitations, including outdated or missing pathway information, and, most importantly, they are not disease specific [8–10]. Thus, the accuracy of the emerging patterns is uncertain and may result in lack of clinical utility for guiding therapy, as has recently been shown by Noor et al. in a study of Crohn's disease where the authors evaluated the classification efficiency of a blood-based biomarker [11]. Thus, more refined and targeted methodologies are necessary for advancing biomarker discovery.

Drug response in the context of UC involves widespread changes in inflammation, and as a result pathways with significant contribution to the treatment response can be overshadowed by inflammatory pathways. In order to unravel the significant contribution of obscured biology, our approach utilizes a murine model coupled with a perturbation source to identify explicit gene expression patterns, and capture underlying mechanisms that represent promising candidates to decipher the lack of response to treatment.

Recent evidence has highlighted the potential involvement of mitochondrial dysfunction in disease severity and treatment response [5], emphasizing the need to identify underlying factors that contribute to mitochondrial dysregulation. In this regard, we have previously described that the absence of Methylation-controlled J protein (MCJ), or DnaJC15, an endogenous negative regulator of mitochondrial complex I, leads to metabolic alterations, increases respiration and adenosine triphosphate (ATP) synthesis and stimulates the formation of respiratory supercomplexes, limiting oxidative stress [12–14]. This qualifies MCJ as a good perturbation source to simulate complex I mitochondrial dysfunction. Our goal was to transfer the findings to human cohorts and assess the persistence of the emerged patterns.

In the context of experimental colitis in a murine model, we have previously shown that deficiency of MCJ contributes to disease severity by modulating the gut microbial composition

146 of the host [15-17]. Moreover, recently we have reported the critical role played by
147 macrophage mitochondrial function in the gut ecological niche, which can substantially affect
148 the severity of inflammation and the ability to successfully respond to anti-TNF therapies [18].
149 The lack of response to the treatment was expressed as an aggravated phenotypic profile,
150 where treated MCJ-deficient mice displayed significantly increased weight loss and
151 histological damage compared to the treated wild-type mice.

152 In the current study, we profiled the transcriptome of colonic tissue from the aforementioned
153 MCJ-deficient murine model of DSS-induced colitis [18], to generate a gene set that captures
154 the relationship between mitochondria dysfunction and lack of response to anti-TNF
155 treatment. Activated monocytes are recruited to the site of inflammation induced by DSS
156 where they differentiate into macrophages. The latter can be polarized towards different
157 subpopulations that can initiate either pro-inflammatory or anti-inflammatory responses [19]. It
158 has been postulated that the FcγR signaling pathway is implicated in the modulation of these
159 diametrically opposed responses [20]. Moreover, it has been suggested that the formation of
160 immune complexes between soluble TNF and therapeutic anti-TNF compounds is necessary
161 for the FcγR-mediated suppression of pro-inflammatory cytokines. We have shown that MCJ
162 expression is restricted to macrophages in colonic tissue, and MCJ-deficiency leads to
163 upregulation of genes belonging to the FcγR signaling pathway and aggravation of the DSS-
164 induced pathology [18]. Thus, we hypothesize that mitochondrial dysregulation can indirectly
165 compromise macrophage function and especially their ability to initiate inflammation-resolving
166 responses.

167 As summarized in Figure 1, we followed a progressive strategy where the captured gene set
168 from the murine model was initially transferred and evaluated in a human cohort that provided

169 transcriptomic data of colonic tissue. Subsequently, we explored whether the captured signal
170 can be detected in blood samples by applying a successive refinement with two human
171 cohorts profiling the transcriptome of peripheral blood monocytes, and whole blood samples.
172 Finally, we utilized an external dataset of whole blood samples from UC patients to evaluate
173 the replication of the findings in blood.

174 This is the first study to use a perturbation source that simulates mitochondrial dysregulation
175 to scrutinize the involvement of the latter on the lack of response to anti-TNF treatment during
176 ulcerative colitis in human patients. Our findings shed new light on the role of metabolic
177 pathways and mitochondrial homeostasis in determining treatment response, and pave the
178 way for further research into the mechanisms underlying anti-TNF response in ulcerative
179 colitis and other inflammatory diseases.

180 Methods

181 Ethics

182 All procedures involving animals, including their housing and care, were carried according to
183 the guidelines of the European Union Council (Directive 2010/63/EU) and Spanish
184 Government regulations (RD 53/2013), and with the approval of the ethics committee of CIC
185 bioGUNE (Spain; permit number CBBA-0615) and the Competent Authority (Diputación de
186 Bizkaia). All human samples were processed within the context of the IBD Sample Collection
187 registered at the HCB-IDIBAPS Biobank and the protocol was approved by the Institutional
188 Ethics Committee of the Hospital Clinic de Barcelona (HCB/2023/0523). Additional approval
189 for the human samples was provided by the Clinical Research Ethics Committee from

190 Euskadi (CEIC-E) following the Helsinki convention (PI2016034). In all human cohorts,
191 patients provided written informed consent following extensive counseling.

192 Animal model and experimental design

193 The murine model [18] included MCJ-deficient (MD) and wild-type (WT) male mice and is
194 referred to as MM dataset herein. To evaluate the response to anti-TNF treatment, colitis was
195 induced in WT and MD mice by administering dextran sodium sulfate (DSS) [15]. The whole
196 experimental period lasted nine days and the mice were divided into two groups per
197 genotype. One group received Infliximab (IFX^+) treatment on the third and sixth day (WT-IFX^+,
198 MD-IFX^+), whereas the second group did not receive the treatment (WT-IFX^-, MD-IFX^-). The
199 distribution of mice per condition was 5 WT (2 WT-IFX^- and 3 WT-IFX^+) and 5 MD mice (2
200 MD-IFX^- and 3 MD-IFX^+). Colon samples were taken from all mice at the end of the
201 experimental period, namely nine days after the treated mice had been administered
202 Infliximab (day-3 and 6), and used to study RNA expression.

203 All procedures and specifications involving animal treatment and the design of the mouse
204 model are described in the supplementary methods (S1).

205 Human cohorts

206 Human cohorts are referred to with the abbreviations COL, MON and BLD. The COL cohort
207 (N=28) included colonic biopsies at week-14 after anti-TNF treatment of UC patients. The
208 MON cohort (N=31) included healthy blood donors and IBD patients that provided monocytes
209 from peripheral blood. The IBD patients were individuals that presented an aggravated state
210 of the disease and either did not respond to previous treatments or manifested severe
211 symptoms. As a result, the IBD patients proceeded to emergency colectomy where blood

212 samples were taken prior to operation. The BLD cohort (N=34) included whole blood samples
213 from UC patients prior to anti-TNF treatment (week-0) and their response was evaluated at
214 week-14. The COL and BLD cohorts provided in total 39 patients, from which 23 patients
215 provided whole blood samples at week-0 and colon samples at week-14, whereas 5 patients
216 provided only colon samples at week-14 and 11 patients only whole blood samples at week-0.
217 Moreover, response to treatment was based on endoscopic activity. Age and gender of
218 patients at inclusion are shown in Table 1 for each cohort. Cohort details and specifications
219 regarding sample collection and treatment are provided in the supplementary methods (S2).

220 RNA extraction, preparation and quantification

221 In the mouse model and human cohorts, gene quantification was performed with RNASeq
222 using the GRCm38 mouse reference and the GRCh38.p13 human reference, respectively. A
223 gene was characterized as differentially expressed (DEG) for a given condition contrast, if it
224 met the following criteria: FDR-corrected p-value (p-adj) ≤ 0.05 and absolute fold-change $|FC|$
225 ≥ 1.5. The derived DEGs were later utilized for enrichment analysis from which only
226 statistically significant enriched pathways were considered (p-adj ≤ 0.05). From each human
227 cohort, the set of significant genes that was selected for downstream analysis was named as
228 COLset, MONset and BLDset denoting the cohort of origin.

229 Detailed specifications regarding RNA extraction and preparation protocols, as well as
230 RNASeq preprocessing and enrichment analysis, are given in the supplementary methods
231 (S3).

232 Incorporation of the Haberman et al. corticosteroid gene signature into the
233 analytical pipeline

234 We incorporated into the analysis the gene signature provided by Haberman et al. [5]. The
235 signature contains 115 genes that resulted from baseline rectal biopsies of 206 pediatric UC
236 patients whose remission status was evaluated on the week-4 of corticosteroid treatment.
237 Notably, this signature exhibited similar classification efficiency in a cohort treated with anti-
238 TNF treatment. From the provided 115 genes, we selected 89 genes that were differentially
239 expressed in our COL cohort. We named the selected genes as HABset, and were used to
240 conduct a comparative assessment with the COLset on their ability to differentiate between
241 responders and non-responders in the COL cohort.

242 Evaluation of the persistence of the captured signal from colon tissue in 243 blood samples

244 Since MCJ expression is restricted in macrophages in colonic tissue [18], we sought to
245 explore whether the captured signal from the COL cohort can be detected in the blood. To do
246 so, we initially identified 48 genes (MONset) in the MON cohort that can distinguish IBD
247 patients from non-IBD individuals. Later, we utilized whole blood samples before treatment
248 from the BLD cohort, where our process for resolving crossover trends between the BLD and
249 MON cohorts provided 14 genes (BLDset) that can classify responders and non-responders
250 IBD patients to treatment. The process followed for the construction of the BLDset is
251 described in the supplementary methods along with the concept of trends (S4).

252 For the classification process in the BLD cohort, we initially regressed-out age and sex from
253 the gene expression data. To avoid overfitting and multicollinearity, we performed PCA on the
254 gene expression and based a non-regularized logistic regression model on the first two PCs
255 with Scikit-learn [21]. One additional advantage of this strategy is that it enables the visual

256 evaluation of the model's performance. To mitigate the impact of the imbalanced conditions,
257 the weights 0.3 and 0.7 were used for the non-responder and responder classes respectively.
258 To evaluate the training process, we performed a 12-fold cross-validation with 3 repeats
259 calculating at each fold the F1-score metric for the BLD training and BLD test-set. The F1-
260 score was chosen since it is a well-suited metric for imbalanced categorical variables. It is
261 interpreted as the harmonic mean of the precision and recall metrics and ranges between 0
262 and 1. Finally, estimation of the decision boundary standard error was based on a
263 bootstrapped 95% confidence interval with 1000 iterations, sampling with replacement and
264 sample size of 34.

265 Replication of the findings in blood with an external dataset

266 To evaluate the replication of the findings in the whole blood, we downloaded the publicly
267 available RNASeq data provided by Mishra *et al.* [22] (GSE191328). It is a blood-based
268 dataset that underwent a similar preprocessing procedure as the BLD cohort, and included
269 three independent cohorts of IBD patients: two that received Infliximab treatment (referred to
270 as discovery and replication cohorts by the authors) and one Vedolizumab. The patients were
271 followed longitudinally from baseline until week-14, where they were classified according to
272 remission status. From the available cohorts, we considered only UC patients and focused on
273 the following time-points: baseline, week-2, week-6 and week-14. The discovery cohort is
274 referred to as IFX (N=9) and the replication cohort as REP (N=9), whereas the Vedolizumab
275 cohort is referred to as VED (N=10) in the current study. To avoid possible integration batch
276 effects and to evaluate patients heterogeneity, we kept the IFX and REP cohorts separate.

277 Prior to model validation, the genes *SLC18A1* and *PPARGC1A* were omitted from the BLDset
278 since they were not quantified across all cohorts and timepoints. We also processed each
279 cohort with DESeq2 stabilizing the gene expression variance with the dispersion function
280 whose parameters were previously estimated with the BLD cohort without specifying patient
281 response. Thus, no patient's response information was introduced during the dispersion
282 estimate that could bias the classification process. Then, each cohort was projected on the
283 PCs that were extracted during the model's training process and the sample scores from the
284 resulting transformation were used as a test-set. Finally, the performance of the classification
285 process in each cohort was assessed using the F1-score metric.

286 Results

287 554 DEGs in the mouse model (MMset) capture the interaction between the 288 absence of MCJ and the response to anti-TNF

289 First, we performed transcriptomic analysis of the colon tissue from a murine model of
290 experimental colitis that included wild-type (WT) and MCJ-deficient (MD) mice. The mouse
291 groups were further subdivided into treated with anti-TNF (WT-IFX$^+$,MD-IFX$^+$) and untreated
292 mice (WT-IFX$^-$,WT-IFX$^-$). As mentioned above, response to anti-TNF treatment was
293 previously evaluated [18]. Similarly to the WT-IFX$^-$ and MD-IFX$^-$ mice, the MD-IFX$^+$ mice
294 displayed an aggravated profile characterized by significantly higher weight loss and
295 histological damage compared to WT-IFX$^+$. Additionally, in the current study we observed
296 high efficiency of the model, with an 8.4-fold and 11.3-fold changes in the mRNA levels of

297 *Dnajc15* between the MD-IFX$^-$ and WT-IFX$^-$ and the MD-IFX$^+$ and WT-IFX$^+$ groups,
298 respectively (Figure S1).

299 To evaluate group differences, we performed principal component analysis (PCA) using all
300 16,186 quantified genes. The MD-IFX$^+$ mice had unique distinguished profiles compared with
301 the other three groups, forming a separate cluster across PC1 (45% of the observed variance,
302 Figure 2A, left plot). The differences between the other three groups appeared weaker,
303 clustering mainly across PC2 (18.8% of the observed variance).

304 Differential gene expression analysis corroborated these observations, with greater intra-
305 group differences within the MD groups than among WT groups. The contrast between MD-
306 IFX$^+$ and MD-IFX$^-$ resulted in 1,544 differentially expressed genes (DEGs), for only 12 DEGs
307 in the WT-IFX$^+$ and WT-IFX$^-$ comparison. Of note, we observed an interaction between
308 *Dnajc15* gene expression and the response to the anti-TNF treatment. Upon administration of
309 Infliximab, 617 genes were differentially expressed between the treated groups (MD-IFX$^+$ and
310 WT-IFX$^+$), for only 12 genes among the corresponding non-treated groups. These
311 observations verify the utility of the mouse model, suggesting a significant interaction between
312 *Dnajc15* expression and the response to Infliximab treatment.

313 We reasoned that the 617 DEGs from the MD-IFX$^+$ versus WT-IFX$^+$ comparison represent a
314 set of genes with the capacity to decipher the mechanisms underlying the relationship
315 between mitochondrial dysregulation and unresponsiveness to the treatment. After removing
316 genes without corresponding human ENSEMBL identification, 554 DEGs were retained,
317 referred to heretofore as the MMset (supplementary materials 1). As expected, PCA showed
318 that the MMset recapitulates the differences between the MD-IFX$^+$ and the other groups,

319 forming a separate cluster across PC1 (72.78% of the observed variance, Figure 2A, right
320 plot).

321 MMset is associated with mitochondrial dysfunction

322 We used MitoMiner's API [23] to identify genes located in the mitochondrion. We identified 50
323 genes from the MMset (supplementary materials 1). These genes had a median 1.21-fold
324 average expression change between the non-treated (WT-IFX$^-$ and MD-IFX$^-$) groups,
325 increasing to 1.86-fold change between the treated groups (Figure S2). These results
326 reinforce the previous idea of an interaction between anti-TNF administration and
327 mitochondrial dysfunction.

328 We identified other notable changes in genes with relevant roles in mitochondrial
329 homeostasis. *Phgdh,* known to compromise the electron transport chain activity and lead to
330 increased production of ROS [22], was significantly down-regulated in the MD-IFX$^+$ group. We
331 observed similar changes for *Hif1a* and *Ripk3*, that play a role in modulating mitochondrial
332 function and metabolism [25,26]. In turn, we observed significant up-regulation of *Ppargc1a*
333 and *Pink1*, which are involved in regulating mitophagy and mitochondrial biogenesis [27].

334 The major enrichment in MMset concerned metabolic pathways

335 To further characterize the biological effects underlying the MMset, we performed enrichment
336 analysis of the full set. Subsets of 107 and 56 genes were associated with metabolic and cell
337 cycle pathways, respectively (supplementary materials 2). From the subset associated with
338 metabolic pathways, 65.4% of the genes were up-regulated in the MD-IFX$^+$ (Figure 2B). In
339 contrast, genes associated with cell cycle pathways were down-regulated in MD-IFX$^+$. The

340 latter represented an interesting observation and we reasoned that the excessive
341 downregulated gene expression concerned cells that had undergone apoptosis. If this
342 rationale holds true, then it is aligned with our hypothesis that mitochondrial dysfunction
343 disrupts the proper function of macrophages to initiate inflammation-resolving processes such
344 as clearance of apoptotic cells.

345 The enrichment of metabolic pathways involved the activation of the xenobiotic response
346 system in the MD-IFX$^+$ group. This includes nuclear receptors that regulate genes involved in
347 the metabolism of xenobiotics, such as the farnesoid X receptor (FXR/*Nr1h4*) that exhibited a
348 1.67-fold change between the MD-IFX$^+$ and WT-IFX$^+$ groups causing the over-expression of
349 the gene *Fabp6*. Moreover, the peroxisome proliferator-activated receptor α (*Ppara*), which
350 regulates the expression of various UGT metabolic enzymes, ABC and SLC transporters, was
351 also found differentially expressed. We also observed up-regulation of the peroxisome
352 proliferator-activated receptor-gamma coactivator (PGC-1/*Ppargc1a*) gene, which interacts
353 with PPARA and together regulate the expression of enzymes involved in the oxidation of
354 mitochondrial fatty acids.

355 MMset signal linking anti-TNF response and mitochondrial dysfunction 356 successfully transferred to a human cohort (COLset)

357 We next analyzed available colon samples from a human UC cohort. Out of 21,780 quantified
358 genes, 3,645 were differentially expressed between responders and non-responders patients.
359 PCA showed a separation between the two groups across PC1, accompanied by an
360 underlying intra-group variability predominantly influenced by PC2 (Figure 3A, “All DEGs”).

361 We then evaluated the expression of genes that could be linked to mitochondrial dysfunction.
362 We used the GeneCards portal [28] to query for genes that are associated with complex I.
363 The search returned 165 genes, of which 25 were differentially expressed (supplementary
364 materials 3). A detailed inspection revealed mitochondrial alterations, with downregulation of
365 complex I activity components such as *MT-ND3*, *MT-ND5*, *MT-ND4*, *MT-ND4L*, *MT-TL1*, and
366 *MT-ND2*, and up-regulation of genes such as *NLRP3*, that gets activated by excessive
367 mitophagy [29], or *DYSF* that regulates cytosolic influx of Ca^{2+} and affects normal
368 mitochondrial function under certain conditions [30].

369 To evaluate the mitochondrial aberrations that were linked to administration of anti-TNF in the
370 murine model, we intersected the 3,645 DEGs with the MMset. This generated a subset of
371 127 DEGs, named COLset (supplementary materials 1). PCA showed that COLset was able
372 to maintain the separation between responders and non-responders and increased the
373 captured observed variance to 70% with the first two PCs (Figure 3A, “COLset”). Interestingly,
374 although *DNAJC15* displayed statistically significant differences between responders and
375 non-responders (p-adj=0.03), its fold-change of 1.3 between the patient groups did not allow it
376 to be considered as differentially expressed and was not included in the COLset. This
377 particular case exemplifies perfectly the potential pitfalls of the typical strategy followed for the
378 discovery of DEGs, as genes that contribute to the underlying mechanism can be overlooked
379 by strict predefined thresholds.

COLset performs similarly to inflammation-driven gene signatures, and shows metabolism as the main enriched pathway

We then juxtaposed the discriminatory capability on the COL cohort of the COLset with a set of 89 genes from the corticosteroid-based gene signature provided recently by Haberman *et al.* [5] that we refer to as the HABset (see methods, supplementary materials 1).

Both gene sets captured above 70% of the observed variance with the first two PCs (Figure 3A), with PC1 scores showing a strong negative Pearson correlation (COLset: r=-0.69, p-value=2.6E-05, HABset: r=-0.70, p-value=2.1E-05) with *DNAJC15* mRNA levels (Figure S3). These results suggest a severity gradient of non-response that correlates with the extent of the underlying MCJ-dependent mitochondrial dysfunction. Nevertheless, both sets shared only 9 genes (*GUCA2B*, *TNIP3*, *SLC26A3*, *VSIG1*, *TRPM6*, *HMGCS2*, *MMP3*, *MMP10* and *CHP2*) suggesting that the two signatures capture different underlying gene expression regulatory components, albeit sharing functional properties.

Indeed, enrichment analysis revealed different captured pathways. The COLset enriched pathways associated with metabolism, transportation of molecules and regulation of nuclear receptors, whereas the HABset appeared linked to pathways related to the immune system, IL-17 signaling and peptide receptors (supplementary materials 2).

Finally, we evaluated the classification efficiency of the two gene sets by constructing two predictive models on the COL cohort (supplementary methods S5). The F1-score was 0.93 with the COLset and 0.97 with the HABset. As a result, the decision boundary separated well the patients groups in both cases (Figure 4). Overall, these two gene sets, although clearly

401 different in regards to gene composition and pathway enrichment, yield similar classification
402 results on samples from colonic tissue from UC patients undergoing anti-TNF treatment.

403 COLset signal was detected in circulating blood monocytes (MONset)

404 We analyzed RNASeq data from peripheral blood monocyte samples with the aim to assess
405 the persistence of the captured signal from the colon samples in the blood. We quantified
406 18,331 genes and identified a set of 9,262 DEGs between healthy non-IBD individuals and
407 IBD patients with a severe disease state that were sampled right before colectomy. The
408 intersection of the latter with the 165 genes related to complex I from GeneCards returned 83
409 genes (supplementary materials 3). Fifty-three genes were up-regulated (FC M=2.89,
410 SD=1.89) and 30 were down-regulated (FC M=2.97, SD=2.15) in the IBD patients. Moreover,
411 the IBD patients exhibited up-regulation of the majority of the NDUF genes that are
412 associated with complex I, and down-regulation of the majority of the TMEM genes that are
413 directly related to ATP synthesis.

414 To associate differential expression related to anti-TNF treatment, we intersected the 9,262
415 DEGs with the COLset, generating a subset of 48 genes which we named as MONset
416 (supplementary materials 1). We attributed the narrow overlap in the homogeneous and
417 purified nature of the samples included in the MON cohort compared to those of the COL
418 cohort. PCA revealed a clear separation between IBD patients and non-IBD individuals,
419 capturing 68% of the observed variance with the first two PCs (Figure 5A). Moreover,
420 enrichment analysis showed metabolism as the sole enriched pathway encompassing 17
421 genes (Figure 5B-C, supplementary materials 2). These results indicate that dysregulated

422 complex I activity can be detected in circulating monocytes, even before they migrate to
423 colonic tissue and differentiate into macrophages.

424 Pre-treatment whole blood samples reveal latent classification signals for 425 UC patient response, linked to mitochondrial dysfunction (BLDset)

426 Following the results from the MON cohort, our next objective was to investigate whether the
427 classification signal of COLset, between responders and non-responders IBD patients, can
428 also be detected in whole blood samples especially before treatment. To do so, we analyzed
429 whole blood samples at baseline of UC patients whose status was identified at a later stage of
430 the treatment (week-14). We quantified 24,039 genes that did not exhibit differential
431 expression between responders and non-responders. The similarity in their transcriptomic
432 profiles at baseline implies that unbiased classification at week-0 through classical gene
433 signature discovery is not possible. However, non-responders displayed a mean of 1.18-fold
434 difference (SD=0.36) compared to responders for the 165 genes associated with complex I
435 from GeneCards (supplementary materials 3). This suggests that perturbations of
436 mitochondrial genes are present before the initiation of the treatment.

437 Due to lack of differential expression in the BLD cohort, it was unfeasible to intersect the
438 COLset with a set of DEGs in the BLD cohort. Therefore, to proceed we utilized the MONset
439 that includes genes from the COLset that exhibit differential expression in the blood.
440 Nevertheless, certain genes from the MONset displayed crossover trends between the BLD
441 and MON cohorts that we attributed to the lack of responders in the MON cohort. Thus, we
442 considered a MONset subset of 14 genes to be included in the classification process which
443 hereafter will be referred to as BLDset (see methods section, supplementary materials 1).

444 During the 12-fold cross-validation of the training process, the classifier achieved a mean F1-
445 score of 0.79 (95% CI: 0.78-0.80) with the BLD training-set, and a mean F1-score of 0.69
446 (95% CI: 0.59-0.79) with the BLD test-set. The panels A and B in Figure 6 depict the decision
447 boundary applied by the classifier and the probability of the assigned class (responder or non-
448 responder) to each included patient.

449 External replication showed attenuated baseline BLDset classification 450 signal in blood, with marked post-treatment improvement

451 To evaluate the replication of the classification process with BLDset, we utilized publicly
452 available blood-based RNASeq data provided recently by Mishra *et al.* [22] (see methods).
453 The study profiled two cohorts that received anti-TNF treatment (IFX and REP) and one
454 cohort that was treated with the $\alpha 4\beta 7$ integrin inhibitor Vedolizumab (VED). Patients were
455 followed longitudinally from baseline until week-14, and the distribution of the patient groups
456 is given in the supplementary methods (S6).

457 At baseline we observed great variability of the classification performance that marked the
458 lowest mean F1-score with the IFX cohort (Figure 7 A-B). However, the classification
459 drastically improved after the initiation of the treatment marking the best performance on
460 week-14. Moreover, we observed that the classification performance for the VED cohort did
461 not follow the same pattern as with the IFX and REP cohorts after baseline, implying
462 specificity of the BLDset towards the anti-TNF treatment.

463 To investigate further the variability in classification performance observed at baseline, we
464 calculated the number of genes with matched ranks (Figure 7A) and trends (Figure 7B)
465 between the BLDset and the external dataset, and compared them to see how they affected

466 the performance. For the IFX cohort, we observed that it showed the highest number of
467 matched ranks with the BLDset, but with only three genes with matched trends. This
468 observation underscored the poor classification performance as compared to the REP and
469 VED cohorts.

470 Although the above observations allowed us to explain the poor performance on the IFX
471 cohort at baseline, the improvement in classification on this cohort at week-6 remained
472 puzzling since the number of matched ranks and trends were relatively the same as in
473 baseline. Initially, we observed that in both timepoints the genes *SLC18A1* and *PIF1*
474 displayed similar trends, and the trend differences concerned the gene *EDN1* (baseline) and
475 *STON1* (week-6) (supplementary Figure S4). We hypothesized that this observation could be
476 associated with latent patterns of gene networks that are associated with the BLD cohort and
477 have been indirectly incorporated in the BLDset and potentially affect the classification in the
478 external dataset. To do so, we initially calculated a mean expression for the BLD cohort
479 concerning the 165 complex I related genes from GeneCards. We then performed the same
480 exercise for each cohort in the external dataset and compared them with the BLD cohort
481 (Figure 7C). Interestingly, we observed that the performance was influenced by the captured
482 state of the patient groups in the BLD cohort regarding these 165 complex I genes. More
483 specifically, the performance improved in cases where the average fold-changes related to
484 these genes between responders and non-responders were closer to those observed in the
485 BLD cohort. Since this could be observed across all timepoints, it corroborated our hypothesis
486 about latent gene networks that can shape the performance of a classifier.

487 # Discussion

488 Mitochondrial genes have recently been highlighted as potentially critical to explain the
489 underlying mechanism that compromises the response to anti-TNF treatments in UC patients.
490 Since such signals could be overshadowed by inflammation-driven pathways, we
491 hypothesized that exploring a mouse model with a clear perturbation source is ideal to
492 unravel obscured biology. In the current study, we first analyzed a murine model of
493 experimental colitis characterized by mitochondrial dysfunction and lack of response to anti-
494 TNF. To simulate a mitochondrial dysfunction, we utilized MCJ deficiency as a perturbation
495 source which is a mitochondrial transmembrane protein that interacts with complex I [12-14].
496 The initial focus was to select a set of genes (MMset) that showed strong relation with
497 mitochondrial dysregulation and response to anti-TNF treatment. Our main goal was to
498 discover underlying expression signals associated with mitochondrial dysfunction that can be
499 hidden by inflammatory pathways.

500 Notably, we also observed deficiency in MCJ expression in the COL cohort, with significant
501 differences between the patient groups. This underscores the relevance of the mouse model
502 with regards to the mitochondrial-driven ability to respond to anti-TNF, and we successfully
503 transferred the classification signal captured by MMset to the COL cohort. The transferred
504 signal (COLset) displayed a significant enrichment of metabolic pathways, and showed
505 classification capacity similar to the recent gene signature provided by Haberman *et al.* [5]
506 (HABset), even though the latter is enriched for inflammation pathways and both sets shared
507 a limited number of genes. This suggests that mitochondrial genes have equal contribution to
508 treatment outcomes as those associated with inflammation. Indeed, compromised
509 mitochondria release damage-associated molecular patterns (DAMPs) and induce innate

510 immune responses [29], establishing an interrelationship between both that could explain the
511 similar classification capacity of COLset and HABset.

512 Given the restricted expression of MCJ to colonic tissue macrophages, it was pertinent to
513 investigate whether the COLset signal extends from the colon to the bloodstream. The MON
514 cohort allowed us to explore this aspect and we identified a significant classification signal
515 (MONset) that was primarily enriched in metabolic pathways. Monocytes are circulating short-
516 lived macrophage precursors that are recruited on demand from the blood to sites of
517 inflammation such as the colon, and our results indicate that circulating monocytes in IBD
518 patients are characterized by compromised complex I activity.

519 Even though classification of pre-treatment response using whole blood samples was not the
520 main focus of this study, the results obtained by the MON cohort prompted us to explore the
521 presence of a classification signal at baseline. Since significant insights from such an exercise
522 can lead to valuable non-invasive classification solutions regarding response, we initially
523 implemented a classification process using the BLD cohort and attempted to replicate the
524 process using an external dataset. Although we did not observe robust performance at
525 baseline, BLDset displayed specificity towards anti-TNF treatment and the whole exercise
526 revealed the impact of gene ranks and trends on the performance across different datasets,
527 as well as the influence of non-DEGs that are involved in the regulatory network. This kind of
528 classification nuances could underlie some of the incongruent results seen in drug response
529 signatures [4,6].

530 The BLDset was the classification signal that persisted from the colon samples to the
531 bloodstream. Its composition included *PPARGC1A*, which is related to mitochondrial
532 biogenesis [5], was found among the highest ranked in expression in most of the cohorts, and

533 is associated with more severe colitis and decreased complex IV activity in knock-out mice
534 [31]. It also included *PHGDH* that has been found to regulate mitochondrial homeostasis [24],
535 and *RASGRF2* that coordinates processes related to the activity of the N-methyl-D-aspartate
536 receptor, which has been reported to induce mitochondrial dysregulation [32]. Other members
537 of the gene set were *SLC18A1*, a transporter with xenobiotic transmembrane activity, the
538 detoxification gene *SULT1A1* [33], *PBLD* that is involved in the inhibition of NF-kB signaling
539 [34] and *LRP8* and *PADI2*, which display calcium-ion activity and could be associated with
540 neoplastic progression in UC [35].

541 We identified certain limitations associated with our study. The small sample size and the
542 imbalanced patient groups limited our ability to optimize the classification process further.
543 This limitation represents an integral part of many studies due to the difficulties of constructing
544 a UC based cohort attributed to the low annual incidence. As a result, the incorporation of
545 patients with Crohn's disease (CD) represents a common workaround in order to increase
546 statistical power. However, CD and UC patients exhibit different transcriptomic profiles [36]
547 and following such strategies increases the risk of introducing additional latent factors into the
548 predictive model. Furthermore, the interaction between gut microbiota and gene expression
549 has not been incorporated into the model, since it would require integration of additional omic
550 data such as metabolomics. There is an interplay between mitochondria and intestinal
551 microbiota, with the latter releasing metabolites that trigger mitochondrial ROS which in turn
552 induce an immune response [15,37]. This interaction may affect the transcriptomic profile of
553 the patients and hence indirectly impact the performance of the classifier.

554 Besides clarifying the molecular mechanisms that underlie the relationship between
555 mithocondrial dysfunction and treatment response, the strategy we followed entails three

insights of interest for future gene signature discovery attempts. First, we show that a well-defined murine model of response to therapy - here in the context of mitochondrial dysfunction - can be representative of response traits observed in patients. Second, the inclusion of a perturbation source allows the identification of key regulatory networks that in other works using standard approaches can be obscured due to major pathways that are captured by enrichment analysis. Third, considering that we leveraged all publicly available longitudinal datasets for the replication of the classification process, our findings raise caution regarding the implementation of classification solutions at baseline, and suggest that more longitudinal studies are needed to characterize well the involved regulatory pathways.

Conclusion

We highlighted the importance of mitochondrial homeostasis in relation to treatment response in the context of UC. Our results indicate that regulatory networks associated with mitochondrial dysfunction can provide promising classification signals that can be detected even in the bloodstream, leading to effective non-invasive classification solutions.

584 **Contributors**

585 LA, UMM conceived and supervised the study. APC, AMC, IS, JC, JP, LGI, IRL, JOZ, MF,
586 IMR, MG, AMA, AS, HR performed experiments and/or provided human samples. LA, JA
587 supervised experiments. DK analyzed data. DK, UMM wrote the manuscript. All authors have
588 reviewed the manuscript.

589

590 **Data sharing statement**

591 The raw transcriptomic data for the mouse model and the COL, MON and BLD human
592 cohorts are publicly available in the SRA repository under the accession number
593 PRJNA1075662.

594

595 **Declaration of interests**

596 The authors declare that the research was conducted in the absence of any commercial or
597 financial relationships that could be construed as a potential conflict of interest.

598

599 **Funding**

600 This work was supported by grants from the Spanish Ministry of Science
601 MCIN/AEI/10.13039/501100011033 (PID2019-108244RA-I00 to UMM, PID2021
602 124328OBI00 to J.A., RYC2020-030632-I to U.M.M, CEX2021-001136-S to U.M.M and D.K),
603 ”la Caixa” Foundation (ID 100010434, fellowship code LCF/BQ/LI18/11630001 to U.M.M), V
604 Grant from GETECCU-MSD (Grupo Español de Trabajo en Enfermedad de Crohn y Colitis
605 ulcerosa to L.A.). A.P.C. and I.S. are supported by fellowships from the University of the
606 Basque Country (UPV/EHU) and the Basque Government, respectively.

607

608 **Acknowledgements**

609

610 We acknowledge all the personnel of the Hospital Clinic IBD Unit (Clinic and laboratory) who
611 participated in patient selection and sample collection, handling and processing and we also
612 thank all the patients who participated in this study and the Research Committee from OSI
613 Barrualde-Galdakao.

614
615
616
617
618
619

620 # References

621

622 1 Roda G, Jharap B, Neeraj N, *et al.* Loss of response to anti-TNFs: Definition,
623 epidemiology, and management. *Clinical and translational gastroenterology* 2016;**7**:e135.

624 2 West NR, Hegazy AN, Owens BM, *et al.* Oncostatin m drives intestinal inflammation
625 and predicts response to tumor necrosis factor–neutralizing therapy in patients with
626 inflammatory bowel disease. *Nature medicine* 2017;**23**:579–89.

627 3 Arijs I, Li K, Toedter G, *et al.* Mucosal gene signatures to predict response to infliximab
628 in patients with ulcerative colitis. *Gut* 2009;**58**:1612–9.

629 4 Verstockt B, Verstockt S, Dehairs J, *et al.* Low TREM1 expression in whole blood
630 predicts anti-TNF response in inflammatory bowel disease. *EBioMedicine* 2019;**40**:733–42.

631 5 Haberman Y, Karns R, Dexheimer PJ, *et al.* Ulcerative colitis mucosal transcriptomes
632 reveal mitochondriopathy and personalized mechanisms underlying disease severity and
633 treatment response. *Nature communications* 2019;**10**:1–3.

634 6 Gaujoux R, Starosvetsky E, Maimon N, *et al.* Cell-centred meta-analysis reveals
635 baseline predictors of anti-TNFα non-response in biopsy and blood of patients with IBD. *Gut*
636 2019;**68**:604–14.

637 7 Biasci D, Lee JC, Noor NM, *et al.* A blood-based prognostic biomarker in IBD. *Gut*
638 2019;**68**:1386–95.

639 8 Wadi L, Meyer M, Weiser J, *et al.* Impact of outdated gene annotations on pathway
640 enrichment analysis. *Nature methods* 2016;**13**:705–6.

641 9 Mubeen S, Tom Kodamullil A, Hofmann-Apitius M, *et al.* On the influence of several
642 factors on pathway enrichment analysis. *Briefings in Bioinformatics* 2022;**23**:bbac143.

643 10 Ma J, Shojaie A, Michailidis G. Network-based pathway enrichment analysis with
644 incomplete network information. *Bioinformatics* 2016;**32**:3165–74.

645 11 Noor NM, Lee JC, Bond S, *et al*. A biomarker-stratified comparison of top-down versus
646 accelerated step-up treatment strategies for patients with newly diagnosed Crohn's disease
647 (PROFILE): a multicentre, open-label randomised controlled trial. *The Lancet*
648 *Gastroenterology & Hepatology*. 2024.

649 12 Hatle KM, Gummadidala P, Navasa N, *et al.* MCJ/DnaJC15, an endogenous
650 mitochondrial repressor of the respiratory chain that controls metabolic alterations. *Molecular*
651 *and cellular biology* 2013;**33**:2302–14.

652 13 Navasa N, Martín I, Iglesias-Pedraz JM, *et al.* Regulation of oxidative stress by
653 methylation-controlled j protein controls macrophage responses to inflammatory insults. *The*
654 *Journal of infectious diseases* 2015;**211**:135–45.

655 14 Barbier-Torres L, Iruzubieta P, Fernández-Ramos D, *et al.* The mitochondrial negative
656 regulator MCJ is a therapeutic target for acetaminophen-induced liver injury. *Nature*
657 *communications* 2017;**8**:1–1.

658 15 Pascual-Itoiz MA, Peña-Cearra A, Martín-Ruiz I, *et al.* The mitochondrial negative
659 regulator MCJ modulates the interplay between microbiota and the host during ulcerative
660 colitis. *Scientific reports* 2020;**10**:1–3.

661 16 Peña-Cearra A, Pascual-Itoiz MA, Lavín JL, *et al.* Mitochondrial complex i dysfunction
662 alters the balance of soluble and membrane-bound TNF during chronic experimental colitis.
663 *Scientific reports* 2022;**12**:1–0.

664 17 Peña-Cearra A, Song D, Castelo J, *et al.* Mitochondrial dysfunction promotes microbial
665 composition that negatively impacts on ulcerative colitis development and progression. *npj*
666 *Biofilms and Microbiomes* 2023;**9(1)**:74.

667 18 Peña-Cearra A, Castelo J, Lavín JL, *et al.* Mitochondrial dysfunction-associated
668 microbiota establishes a transmissible refractory response to anti-TNF therapy during
669 ulcerative colitis. *Gut Microbes* 2023;**15(2)**:2266626.

670 19 Anderson CF, Mosser DM. Cutting edge: biasing immune responses by directing antigen
671 to macrophage Fcγ receptors. *The Journal of Immunology*. 2002;**168(8)**:3697-701.

672 20 Bloemendaal FM, Koelink PJ, van Schie KA, *et al*. TNF-anti-TNF immune complexes
673 inhibit IL-12/IL-23 secretion by inflammatory macrophages via an Fc-dependent mechanism.
674 *Journal of Crohn's and Colitis*. 2018;**12(9)**:1122-30.

675 21 Pedregosa F, Varoquaux G, Gramfort A, *et al.* Scikit-learn: Machine learning in Python.
676 *Journal of Machine Learning Research* 2011;**12**:2825–30.

677 22 Mishra N, Aden K, Blase JI, *et al.* Longitudinal multi-omics analysis identifies early
678 blood-based predictors of anti-TNF therapy response in inflammatory bowel disease. *Genome*
679 *medicine* 2022;**14**:1–20.

680 23 Smith AC, Robinson AJ. MitoMiner v3.1, an update on the mitochondrial proteomics
681 database. *Nucleic acids research* 2016;**44**:D1258–61.

682 24 Vandekeere S, Dubois C, Kalucka J, *et al.* Serine synthesis via PHGDH is essential for
683 heme production in endothelial cells. *Cell metabolism* 2018;**28**:573–87.

684 25 Choudhry H, Harris AL. Advances in hypoxia-inducible factor biology. *Cell metabolism*
685 2018;**27**:281–98.

686 26 Islam T, Afonso MB, Rodrigues CM. The role of RIPK3 in liver mitochondria
687 bioenergetics and function. *European Journal of Clinical Investigation* 2022;**52**:e13648.

688 27 Novak EA, Mollen KP. Mitochondrial dysfunction in inflammatory bowel disease.
689 *Frontiers in cell and developmental biology* 2015;**3**:62.

690 28 Safran M, Dalah I, Alexander J, *et al.* GeneCards version 3: The human gene
691 integrator. *Database* 2010;**2010**.

692 29 Chen G, Kroemer G, Kepp O. Mitophagy: An emerging role in aging and age-
693 associated diseases. *Frontiers in cell and developmental biology* 2020;**8**:200.

694 30 Vincent AE, Rosa HS, Alston CL, *et al.* Dysferlin mutations and mitochondrial
695 dysfunction. *Neuromuscular Disorders* 2016;**26**:782–8.

696 31 Cunningham KE, Vincent G, Sodhi CP, *et al.* Peroxisome proliferator-activated
697 receptor-γ coactivator 1-α (PGC1α) protects against experimental murine colitis. *Journal of*
698 *Biological Chemistry* 2016;**291**:10184–200.

699 32 Gao X, Xu X, Pang J, *et al.* NMDA receptor activation induces mitochondrial
700 dysfunction, oxidative stress and apoptosis in cultured neonatal rat cardiomyocytes.
701 *Physiological research* 2007;**56**:559.

702 33 Langmann T, Moehle C, Mauerer R, *et al.* Loss of detoxification in inflammatory bowel
703 disease: Dysregulation of pregnane x receptor target genes. *Gastroenterology* 2004;**127**:26–
704 40.

705 34 Chen S, Liu H, Li Z, *et al.* Epithelial PBLD attenuates intestinal inflammatory response
706 and improves intestinal barrier function by inhibiting NF-κb signaling. *Cell death & disease*
707 2021;**12**:1–5.

708 35 Brentnall TA, Pan S, Bronner MP, *et al.* Proteins that underlie neoplastic progression of
709 ulcerative colitis. *PROTEOMICS–Clinical Applications* 2009;**3**:1326–37.

710 36 Yang L, Tang S, Baker SS, *et al.* Difference in pathomechanism between crohn's
711 disease and ulcerative colitis revealed by colon transcriptome. *Inflammatory bowel diseases*
712 2019;**25**:722–31.

713 37 Özsoy M, Stummer N, Zimmermann FA, *et al.* Role of energy metabolism and
714 mitochondrial function in inflammatory bowel disease. *Inflammatory Bowel Diseases*
715 2022;**28**:1443–50.

716

717

718

719

720

721

722

Figures

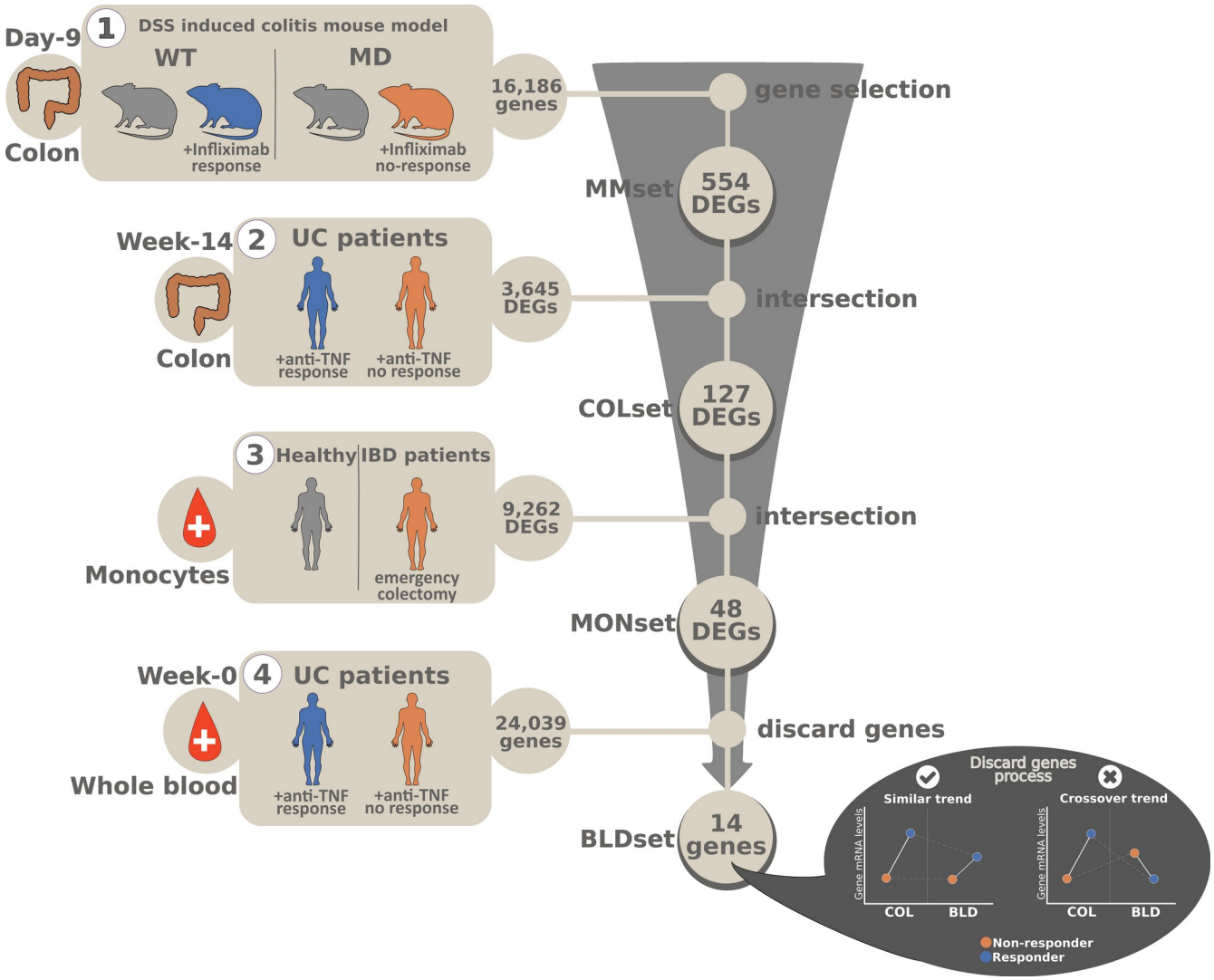

Figure 1: Experimental design. **Phase 1**: The analysis was based initially on a murine model of experimental DSS induced colitis characterized by MCJ-deficiency (MD) and mitochondrial complex I dysfunction. A set of 554 genes (MMset) was selected that showed strong relation with mitochondrial genes and response to anti-TNF treatment. **Phase 2**: We transferred the captured signal to a human cohort of UC patients that was treated with anti-TNF and provided colon samples. We identified a set of 127 genes (COLset) that match differential expression in MMset. **Phase 3**: We identified a classification signal of 48 genes (MONset) from the COLset that can be detected in circulating monocytes by comparing healthy individuals and IBD patients with an aggravated state of the disease that proceeded to emergency colectomy. **Phase 4**: Using whole blood samples of UC patients before anti-TNF treatment, we identified

a signal of 14 genes from MONset (BLDset). The 14-gene based BLDset became the input of a classification process regarding response before anti-TNF treatment.

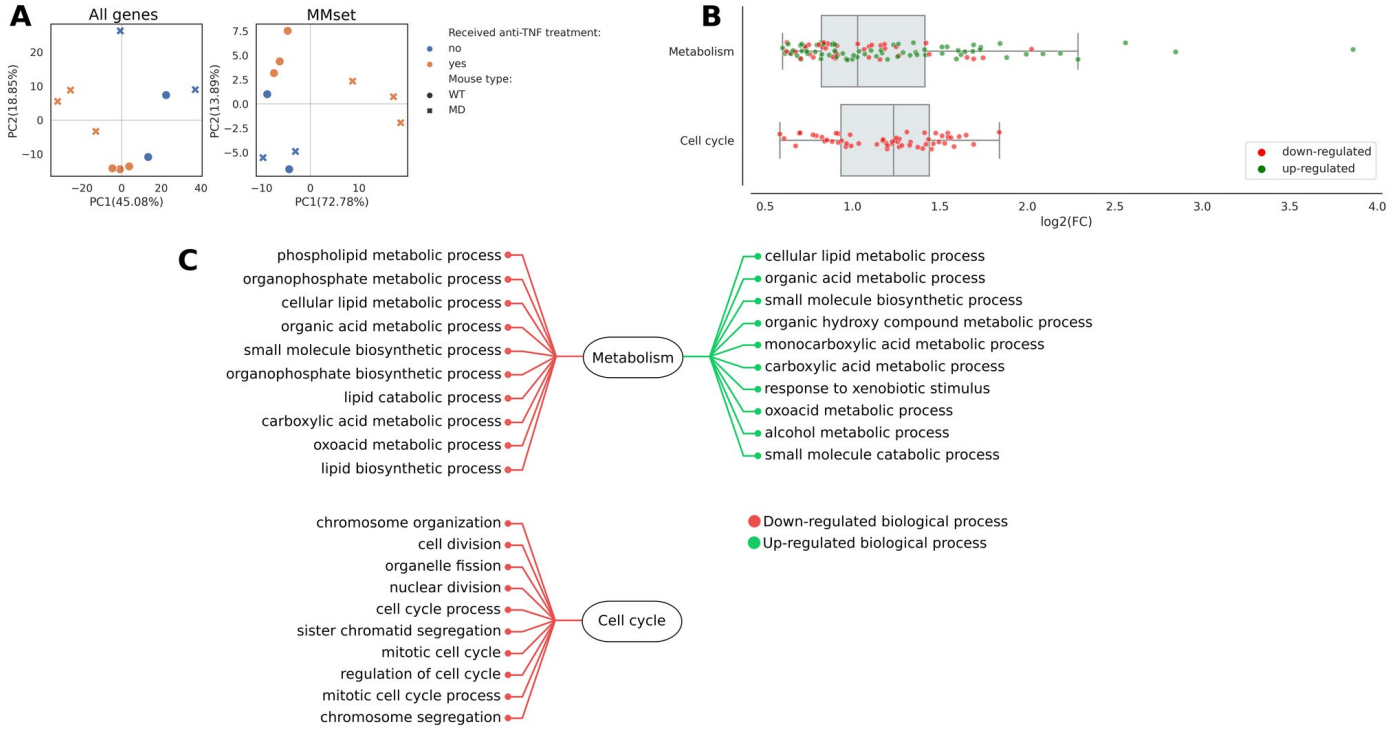

Figure 2: A) PCA using all 16,186 quantified genes (left) from the mouse model or only the MMset (right). **B)** Distribution of log2-fold changes (x-axis) between MD-IFX+ and WT-IFX+ for each enriched pathway based on MMset. In each pathway, up and down-regulated genes are indicated for the MD-IFX+ in relation to WT-IFX+ group. **C)** Up and down-regulated biological process related to each enriched pathway. Regulation is indicated for MD-IFX+ in relation to WT-IFX+ group.

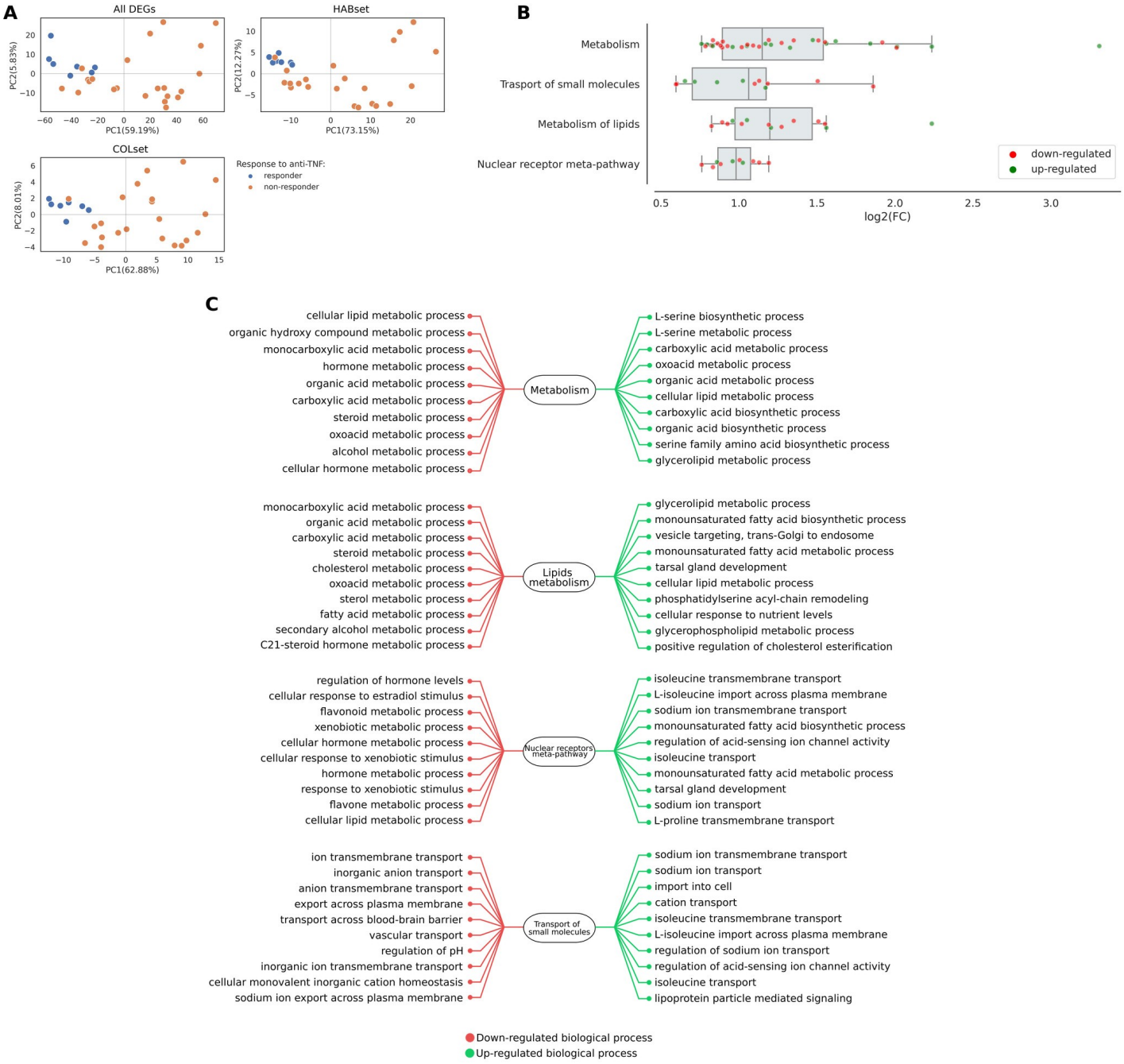

Figure 3: A) PCA using either all 3,645 genes that were differentially expressed between responders and non-responders to anti-TNF UC patients, HABset or COLset. **B)** Distribution of log2-fold changes (x-axis) between responders and non-responders to anti-TNF for each enriched pathway based on COLset. In each pathway, up and down-regulated genes are indicated for non-responders in relation to responders to anti-TNF UC patients. **C)** Up and

down-regulated biological process related to each enriched pathway. Regulation is indicated for non-responders in relation to responders to anti-TNF UC patients.

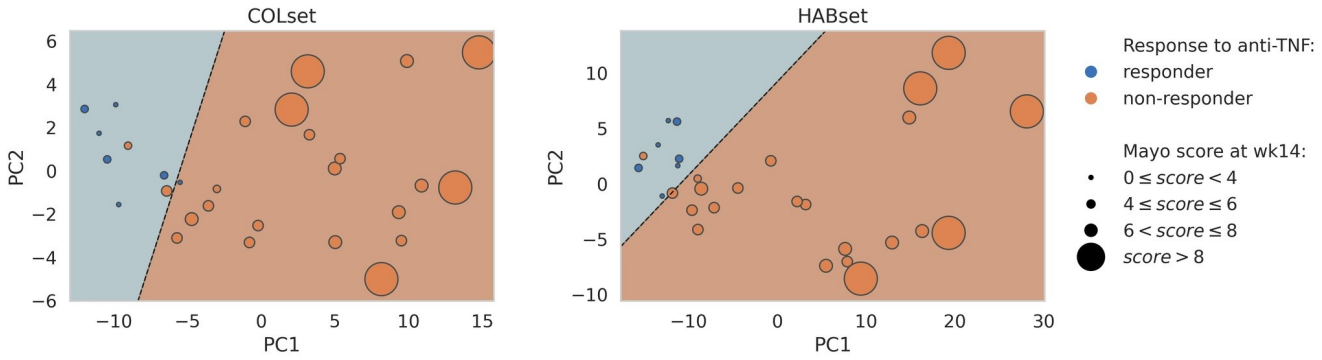

Figure 4: Performance of the anti-TNF logistic regression classifier based on the COL cohort and the first two PCs of the corresponding PCA that was performed using the COLset (left) or the HABset (right). Dashed line represents classifier's decision boundary. Patients to the right side of the decision boundary (shaded orange) have been classified as non-responders by the model, whereas to the left side (shaded blue) as responders to anti-TNF. Patients have been annotated based on their observed response (color) and assigned endoscopic Mayo score (size).

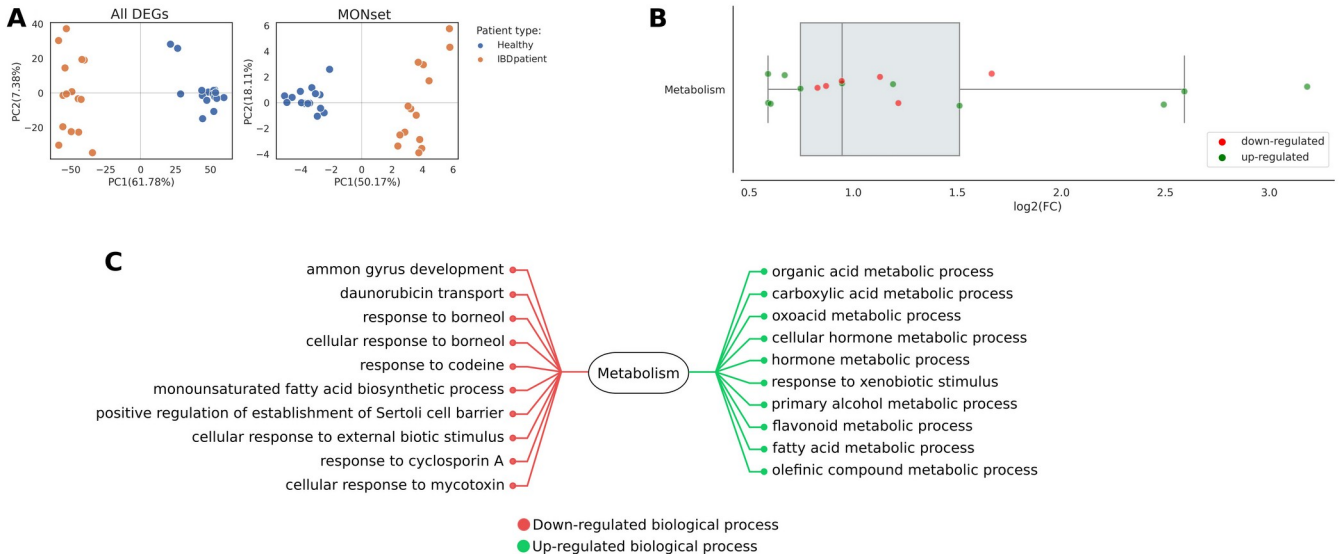

Figure 5: A) PCA using all 9262 genes that were differentially expressed between healthy and IBD patients or genes included in the MONset. **B)** Distribution of log2-fold changes (x-axis) between healthy individuals and IBD patients based on MONset. In each pathway, up and down-regulated genes are indicated for the IBD patients in relation to healthy individuals. **C)** Up and down-regulated biological process related to each enriched pathway. Regulation is indicated for IBD patients in relation to healthy individuals.

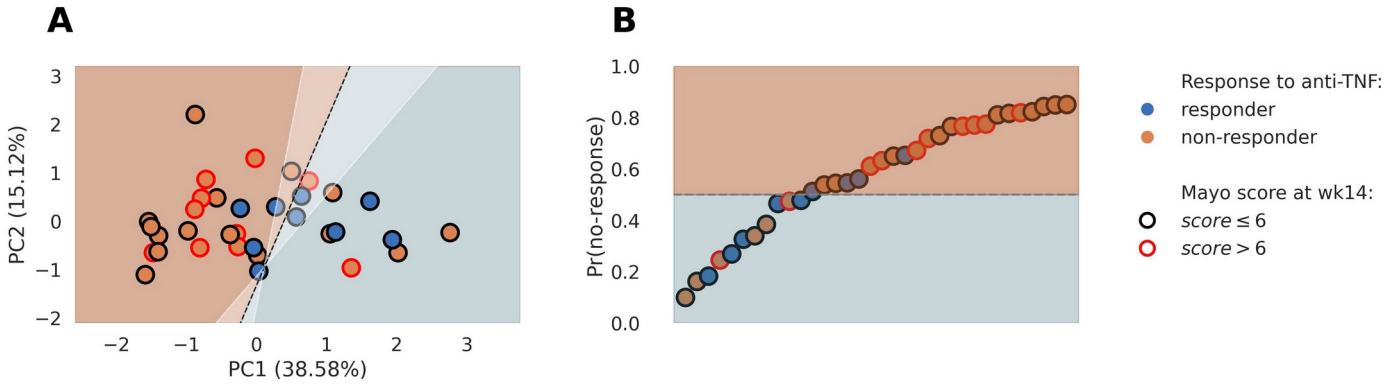

Figure 6: A) Performance of the anti-TNF logistic regression classifier based on the BLD cohort and the first two PCs of the corresponding PCA that was performed using the 14 genes of BLDset. Dashed line represents classifier's decision boundary. White shaded area around decision boundary represents bootstrapped 95% CI, associated with the range within which the decision boundary could be positioned. Patients to the right side of the decision boundary (shaded orange) have been classified as non-responders by the classifer, whereas to the left side (shaded blue) as responders to anti-TNF. **B)** the probabilities assigned by the

classifer to each patient are given, regarding the possibility of no-response to anti-TNF treatment using the BLDset. The classifier implements a probability threshold (decision boundary) of ≥50% to classify a patient as non-responder (shaded orange area) and <50% as responder to anti-TNF (shaded blue area). In all graphical representations, patients have been annotated based on observed response at week-14 after treatment (color) and assigned endoscopic Mayo score (outline).

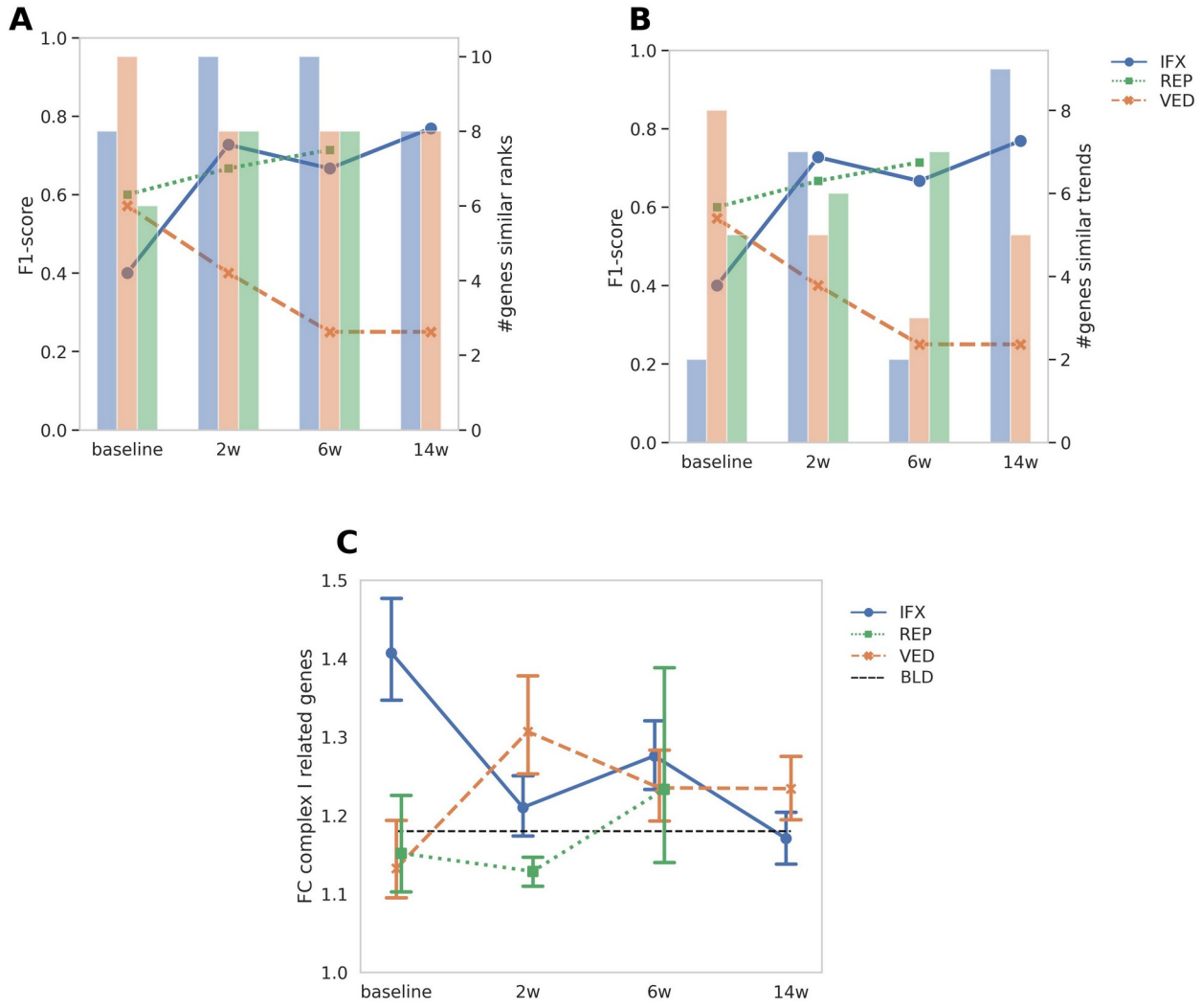

Figure 7: A) Lines represent F1-score achieved by the classifier for the cohorts that received anti-TNF (IFX, REP) or Vedolizumab (VED). Bars represent the numbers of BLDset genes from the corresponding cohorts that received the same rank as those in the BLD cohort. **B)** Lines represent F1-score achieved by the classifier for the cohorts that received anti-TNF (IFX, REP) or Vedolizumab (VED). Bars represent the number of BLDset genes from the

corresponding cohorts that exhibit similar trend between patients groups when compared with those in the BLD cohort. **C)** For each cohort and time-point, the mean fold-change between the responders and non-responders UC patients is shown (error bars denote standard deviation), concerning 165 genes related to complex I. Black horizontal line represents the corresponding mean fold-changes that were observed in the BLD cohort. In all graphical representations, samples at week-14 were not available for the REP cohort.

Tables

	N	Age (MIN-MAX)	Gender (F/M)
		COL cohort	
responders UC	7	41 (20-60)	3/4
non-responders UC	21	46 (27-70)	9/12
		MON cohort	
healthy	16	N/A (18-65)	N/A
IBD patients	15	49 (23-77)	4/11
		BLD cohort	
responders UC	9	49 (24-87)	3/6
non-responders UC	25	53 (32-78)	11/14

Table 1: Human cohorts specifications. Age is reported based on average and observed minimum and maximum values. Information regarding average age and gender was not available for the healthy individuals in the MON cohort.

Supplementary Materials

Materials 1

List of genes that were included in MMset, COLset, HABset, MONset and BLDset.

Materials 2

Pathway enrichments for genes included in the MMset, COLset, HABset and MONset.

Materials 3

List of complex I related genes that were differentially expressed in COL and MON cohorts.